

Lateral organization of mixed, two-phosphatidylcholine liposomes as investigated by GPS, the slope of Laurdan generalized polarization spectra

Alba A. Vallejo, Jesús B. Velázquez¹, Marta S. Fernández *

Department of Biochemistry, Centro de Investigación y de Estudios Avanzados del I.P.N. (CINVESTAV),
P.O. Box 14.740, 07000 México D. F., Mexico

Received 18 June 2007, and in revised form 29 June 2007
Available online 10 July 2007

Abstract

The effect of the excitation or emission wavelengths on Laurdan generalized polarization (GP) can be evaluated by GPS, a quantitative, simplified determination of the GP spectrum slope, the thermotropic dependence of which allows the assessment of phospholipid lamellar membrane phase, as shown in a recent publication of our laboratory [J.B. Velázquez, M.S. Fernández, *Arch. Biochem. Biophys.* 455 (2006) 163–174]. In the present work, we applied Laurdan GPS to phase transition studies of mixed, two-phosphatidylcholine liposomes prepared from variable proportions of dimyristoyl- and dipalmitoylphosphatidylcholine (DMPC and DPPC, respectively). We have found that the GPS function reports a clear limit between the gel/liquid-crystalline phase coexistence region and the liquid-crystalline state, not only at a certain temperature T_c for liposomes of constant composition submitted to temperature scans, but also at a defined mole fraction X_c , for two-component liposomes of variable composition at constant temperature. The T_c or the X_c values obtained from GPS vs. temperature or GPS vs. composition plots, respectively, allow the construction of a partial phase diagram for the DMPC–DPPC mixtures, showing the boundary between the two-phase coexisting region and the liquid-crystalline state. Likewise, at the onset of the transition region, i.e., the two-phase coexisting region as detected by GPS, it is possible to determine, although with less precision, a temperature T_o or a mole fraction X_o defining a boundary located below but near the limit between the gel and ripple phase, reported in the literature. These GPS results are consistent with the proposal by several authors that a fraction of L_α phospholipids coexists with gel phospholipids in the rippled phase.

© 2007 Elsevier Inc. All rights reserved.

Keywords: Laurdan; GPS; Generalized polarization spectrum slope; DMPC–DPPC liposomes; Phase transition; Ripple phase

Cumulative evidence over the last three decades, points to heterogeneities in the lipid matrix of biological membranes as playing important roles in many cellular processes. These processes include, among others, the membrane function of enzymes, transporters and channels as well as the location and redistribution of receptors or sites for virus entry and budding [1,2]. Lipid membrane heterogeneities are likely to be related to phase separation phenomena [3]. Still, the physical behavior of complex mix-

tures of membrane lipids is not completely understood. It is obvious that a better knowledge of lipid miscibility or phase separation needs more studies using model systems. Consistent with this, we are seeing a revival of the classical model membrane studies of the seventies [4,5], updated by use of current approaches and methodologies [6–11].

Much of the work in our laboratory is and has been concerned with model membranes. Our interests range from the analysis of lipid surface ionization in bilayers [12–14] to studies of the effect of liposome physical state on the interfacial activation of phospholipase A₂ [15–18]. In fact, the interfacial activation of this enzyme is extremely sensitive to the fine morphological details of the organized

* Corresponding author. Fax: +52 55 5061 3391.

E-mail address: msfernandez@cinvestav.mx (M.S. Fernández).

¹ Present address: Universidad Aut. Nayarit, Tepic, C.P. 63155, Mexico.

substrate, as recently shown by Leidy et al. [19]. Such a conclusion comes from atomic force microscopy observations of the hydrolysis of ripple-phase supported bilayers, for which the coexistence of a fraction of liquid-crystalline phospholipids with a predominantly gel matrix, has been proposed [19,9]. The study relied on the use of substrate bilayers composed of DMPC² and distearoylphosphatidylcholine, two phospholipids which are not completely miscible [19]. This is only one of many lines of evidence indicating that the issues of phase coexistence and phase miscibility of lipids can provide a better understanding of biologically relevant interfacial phenomena.

One of the simplest but most informative systems in the investigation of the lateral organization of lipids is the binary phospholipid model membrane composed of DMPC and DPPC which can be taken as model of near-ideal mixing behavior. This phospholipid combination, however, also shows phase coexistence in certain regions of its temperature–composition phase diagram, particularly in the phase transition region [4,5,20–22].

In the last years, significant information on the physical properties of membranes and specifically, on the lateral organization of lipids, has been obtained using the fluorescence monitor Laurdan [11,23–30,35]. Thanks to its solvatochromic properties [31], this probe yields emission spectra revealing substantial differences between the gel and liquid-crystalline phases. In the latter case, there is dipolar relaxation of water around Laurdan in the excited state, a mechanism that is barely effective in the gel phase. Therefore, emission spectra are shifted to higher wavelengths in the liquid-crystalline state with respect to the gel phase, a shift that is conveniently described by GP, the generalized polarization function first described by Parasassi, Gratton and coworkers [23–30]. In addition, Laurdan GP shows sensitivity to the excitation and emission wavelengths depending on the phase state of the lipid environment in which the monitor is immersed. As a consequence, different responses are found in phase coexistence, gel or liquid-crystalline states [11,23,24,28–30,32–34]. To evaluate these wavelength effects we have recently introduced the function GPS, the slope of Laurdan generalized polarization spectra [11]. This function provides a simplified estimation of the slopes and reflects quantitatively the effect of excitation or emission wavelengths on

Laurdan generalized polarization (GP). The thermotropic profile of GPS can be used to define the physical state of lipid membranes. It allows the detection of the apparent limit between the two-phase coexistence region and the liquid-crystalline state in lamellar systems at a well defined temperature point that we have designated as T_c [11]. It also allows the identification, although with less precision, of another temperature T_o , in the limit between the gel phase and the two-phase coexisting region.

Our previous study of the GPS function was conducted on single, pure phospholipid liposomes and vesicles from *Escherichia coli* lipid extracts [11]. The present research attempts to further validate the use of the GPS approach to detect phase transitions in lamellar systems. To this purpose we extend the application of GPS to the analysis of the fluorescence behavior of Laurdan incorporated into binary liposomes composed of DMPC and DPPC. In this way, the GPS function can be tested under the controlled conditions of a binary system in which the proportions of the components are gradually changed. The specific aims are threefold. First, to study the phase properties of mixed liposomes of DMPC and DPPC at different mole fractions, by means of the thermotropic profiles of Laurdan GPS, the generalized polarization spectrum slope. Second, to investigate whether GPS is sensitive to isothermal, compositional induced phase changes of the DMPC–DPPC liposomes. Third, to analyze the possible correlation between our GPS-derived phase transition parameters and published data from the literature, in terms of temperature–composition phase diagrams for the binary system.

Materials and methods

Materials

The fluorescent monitor Laurdan was purchased from Molecular Probes. The synthetic phospholipid 1,2-dimyristoyl-*sn*-glycero-3-phosphatidylcholine and 1,2-dipalmitoyl-*sn*-glycero-3-phosphatidylcholine were from Sigma Chemical Company and their nominal purity, reported to be higher than 99%, was checked by thin-layer chromatography using silica gel plates and chloroform/methanol/acetic acid/water (140:40:16:8 v/v) as developing solvent. No impurities were detected in the plates when visualized under UV light after being sprayed with 0.1% ANS (8-anilino-1-naphthalenesulfonic acid, sodium salt) aqueous solution [36]. Only spectroscopic grade solvents were employed. All other reagents were analytical grade. Triple distilled water was further purified by ultrafiltration through a Milli-Q system from Millipore.

Liposome preparation

Liposomes were prepared as described previously [11–18], by sonication and further annealing about 10 °C above the T_m of the phospholipid or phospholipid mixture employed. The procedure is described in brief. Appropriate volumes of chloroform/methanol (9:1, v/v) solutions of each phosphatidylcholine to give the required working phospholipid concentrations, were thoroughly mixed and thereafter, the organic solution was evaporated with a nitrogen stream. In order to remove any possible trace of retained chloroform, the lipid sample was redissolved in cyclohexane and redried exhaustively with nitrogen. The dry lipids, resuspended in an adequate volume of 10 mM Tris–HCl, NaCl 10 mM, CaCl₂ 5 mM, pH 8.0, at a total concentration of 0.1 mM, were cosonicated using a 20-kHz B30

² Abbreviations used: Laurdan, 6-lauroyl-2-dimethylaminonaphthalene; DMPC, 1,2-dimyristoyl-*sn*-glycero-3-phosphatidylcholine; DPPC, 1,2-dipalmitoyl-*sn*-glycero-3-phosphatidylcholine; GP, generalized polarization; GPS, generalized polarization spectrum slope; GP_{exc}S, generalized polarization excitation spectrum slope; GP_{em}S, generalized polarization emission spectrum slope; T_o , temperature defining the limit between gel phase and phase coexistence in a GPS thermotropic profile; T_c , temperature defining the limit between phase coexistence and liquid crystalline phase in a GPS thermotropic profile; X_o , mole fraction defining the limit between gel phase and phase coexistence in a GPS vs. composition plot for DMPC–DPPC liposomes; X_c , mole fraction defining the limit between phase coexistence and liquid crystalline phase in a GPS vs. composition plot for DMPC–DPPC liposomes.

Branson sonifier cell disruptor in the pulsed mode at 70% duty cycle (actual sonication time: 42 min) followed by 1 h annealing. Liposomes were labeled by adding Laurdan to a final concentration of 0.3 μM from a stock solution of the probe in dimethylsulfoxide. Addition was performed quickly while shaking the sample in a vortex stirrer. After 2 min shaking, the samples were magnetically stirred for 1 h in the dark, before initiating the fluorescence measurements [11]. The fluorophore to lipid ratio was 1:333.

Fluorescence studies

Fluorescence measurements were performed in a Perkin-Elmer Luminescence LS50B Spectrophotometer equipped with a magnetically stirred, thermostatted sample chamber. Temperature was recorded continuously by means of a Teflon covered IT18 microprobe thermocouple inserted directly into the cuvette and connected to a Bailey digital thermometer. The target sample temperature was approached upwards and kept constant for 5 min before reading the fluorescence. Spectra acquisition was done at a speed of 50 nm min^{-1} . For the analysis of data the FL Winlab software was employed. Fluorescence measurements were corrected for light scattering by subtraction of appropriate blanks from the readings [11].

Analysis of fluorescence measurements and calculation of GP, the generalized polarization of Laurdan

When Laurdan is inserted in liquid-crystalline membranes its fluorescence is displaced about 50 nm to higher wavelengths as compared to the emission in the gel phase [26]. The generalized polarization (GP), as defined by Parasassi and coworkers [23–30], is calculated from the fluorescence intensities at wavelengths near Laurdan emission maxima in the gel and liquid-crystalline states. In the case of the excitation generalized polarization ($\text{GP}_{\text{exc}}^{\lambda}$), the following equation can be applied [11]:

$$\text{GP}_{\text{exc}}^{\lambda} = \frac{I_{440} - I_{490}}{I_{440} + I_{490}} \quad (1)$$

where I_{440} and I_{490} are the fluorescence intensities at 440 and 490 nm, corresponding to the gel and liquid-crystalline phases, respectively, upon excitation at a fixed wavelength λ . In the gel phase, where practically no solvent relaxation occurs, $I_{440} > I_{490}$ whereas in the liquid-crystalline state, due to reorientation of water around the excited fluorophore, $I_{440} < I_{490}$ [26,28,33]. Likewise, the expression employed to calculate the emission generalized polarization ($\text{GP}_{\text{em}}^{\lambda}$), is:

$$\text{GP}_{\text{em}}^{\lambda} = \frac{I_{410} - I_{340}}{I_{410} + I_{340}} \quad (2)$$

where I_{410} and I_{340} are the fluorescence intensities near the fluorophore excitation maxima in gel and liquid-crystalline phases, respectively, at the fixed emission wavelength λ [11]. It should be noted that in the gel phase, $I_{410} > I_{340}$ while in the liquid-crystalline state, $I_{410} < I_{340}$. This opposite behavior has been attributed to photoselection of the Laurdan fluorophores surrounded by gel phase phospholipids [26,28,33].

The effect of wavelength on generalized polarization. Calculation of GPS, the slope of generalized polarization spectra of Laurdan

The wavelength dependence of GP is related to the physical state of the bilayer in which Laurdan is inserted [23,24,28–30,32–34]. In a previous paper from our laboratory we quantified the effect of the variation of excitation or emission wavelengths on GP as a diagnostic test of lipid phase state [11]. The test can be performed by two procedures that yield comparable results. The first one requires obtaining the excitation and emission GP spectra. The excitation GP spectrum is constructed by applying Eq. (1) to every excitation wavelength value (λ) in the range $340 \text{ nm} \leq \lambda \leq 410 \text{ nm}$. For the generalized polarization emission spectrum Eq. (2) is applied to each emission wavelength value (λ) in the range $440 \text{ nm} \leq \lambda \leq 490 \text{ nm}$. Thereafter, first order regression lines are fitted to the experimental points of the $\text{GP}_{\text{exc}}^{\lambda} = f(\lambda_{\text{exc}})$ and $\text{GP}_{\text{em}}^{\lambda} = f(\lambda_{\text{em}})$ plots,

and the slopes are determined. For the second procedure we have introduced the quantification of GPS, the average slope of GP vs. wavelength, through a linear model function [11]. In this way data are collected at a combination of two fixed excitation or emission wavelengths. The excitation GP spectrum slope ($\text{GP}_{\text{exc}}^{\lambda}\text{S}$) and the emission GP spectrum slope ($\text{GP}_{\text{em}}^{\lambda}\text{S}$) are calculated by means of Eqs. (3) and (4), respectively, as indicated below. To analyze the dependence of $\text{GP}_{\text{exc}}^{\lambda}$ upon the excitation wavelength (λ_{exc}), $\text{GP}_{\text{exc}}^{\lambda}\text{S}$, was quantified between 340 and 410 nm:

$$\text{GP}_{\text{exc}}^{\lambda}\text{S} = \frac{\text{GP}_{\text{exc}}^{410} - \text{GP}_{\text{exc}}^{340}}{410 - 340} \text{ nm}^{-1} \quad (3)$$

In the case of the $\text{GP}_{\text{em}}^{\lambda}\text{S}$ dependence on λ_{em} , $\text{GP}_{\text{em}}^{\lambda}\text{S}$ was calculated between 440 and 490 nm:

$$\text{GP}_{\text{em}}^{\lambda}\text{S} = \frac{\text{GP}_{\text{em}}^{490} - \text{GP}_{\text{em}}^{440}}{490 - 440} \text{ nm}^{-1} \quad (4)$$

Results

Laurdan GPS in the study of the thermotropic behavior of DMPC–DPPC mixed liposomes

GPS, the slope of the generalized polarization vs. wavelength plot, gives information about the phase state of a lamellar system. For $\text{GP}_{\text{exc}}^{\lambda}$ spectra, a negative slope is linked to liquid-crystalline state and a positive slope to phase coexistence. In the case of the $\text{GP}_{\text{em}}^{\lambda}$ vs. wavelength plot, a positive slope indicates liquid-crystalline phase and a negative slope coexisting phases [23,24,28–30,32–34]. In both $\text{GP}_{\text{exc}}^{\lambda}$ and $\text{GP}_{\text{em}}^{\lambda}$ spectra, a zero slope may correspond to the gel state or, as we have found recently, to the apparent limit between phase coexistence and liquid-crystalline state. This limit, located at the intersection of GPS with the temperature axis, is designated as T_c [11].

An initial approach to the study of Laurdan GPS behavior in mixed liposomes was to investigate a 1:1 DMPC–DPPC mixture. Fig. 1 depicts the effect of temperature

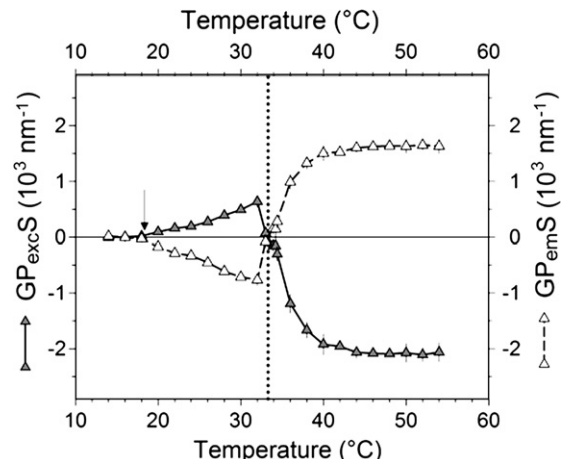


Fig. 1. Effect of temperature on $\text{GP}_{\text{exc}}^{\lambda}\text{S}$ (—▲—) and $\text{GP}_{\text{em}}^{\lambda}\text{S}$ (---△---) of Laurdan in 1:1 DMPC–DPPC liposomes. $\text{GP}_{\text{exc}}^{\lambda}\text{S}$ and $\text{GP}_{\text{em}}^{\lambda}\text{S}$ have been calculated through Eqs. (3) and (4). Results are the means ($\pm \text{SD}$) of three experiments. The vertical dotted line corresponds to $T_c = 33.3 \text{ }^\circ\text{C}$ and marks the apparent boundary between the two-phase coexistence region and the liquid-crystalline state. The arrow pointing at $18.1 \text{ }^\circ\text{C}$ shows T_o , the limit between gel and phase coexistence region.

on GP_{exc}^S and GP_{em}^S for Laurdan incorporated into the two-component vesicles as calculated through the two-point equations (Eqs. (3) and (4)). At low temperatures the curve shows GP_{exc}^S values close to zero corresponding to the gel phase. As the temperature is raised GP_{exc}^S increases as expected for phase coexistence and then, drops abruptly, intersects the temperature axis and reaches the negative values typical of liquid-crystalline state. Concerning GP_{em}^S , it is close to zero at the low temperatures of gel phase, decreases towards negative values in phase coexistence and then rises again, intersects sharply the temperature axis and becomes positive in the liquid-crystalline state. Interestingly, the intersections of GP_{exc}^S and GP_{em}^S with the abscissa are nearly coincident such that the same temperature of inversion of the GPS sign is obtained. This behavior, which is similar to that of pure phospholipids and phospholipid extracts of *E. coli* grown at 45 °C [11], facilitates the precise detection of T_c in studies of the thermotropic phase changes of membranes. In the experiment of Fig. 1, the inversion temperature T_c is 33.3 °C, as indicated by the vertical, dotted line. Another characteristic point detected by Laurdan GPS is T_o , the temperature at the onset of the phase transition in a heating scan, marking the limit between the pure gel state and the region of gel and liquid-crystalline coexisting phases. This point is around 18 °C for the DMPC–DPPC 1:1 mixture, as denoted by the arrow. Such temperature at the edge of the gel phase cannot be distinguished as clearly as T_c because the change from the gel phase to the coexistence region takes place smoothly. It can be observed that GPS fluctuates around zero for the gel phase and then, driven by the increase in temperature, gradually takes the values typical of coexisting phases which are negative for GP_{em}^S and positive for GP_{exc}^S . This difference in the precision of measurements may result in larger standard deviations for T_o values as compared to T_c values.

The GPS thermotropic profile can also be obtained from linear regression analysis of the excitation and emission GP spectra, at different temperatures. The results are presented in Fig. 2 where the upper panel (panel A) displays the wavelength dependence of Laurdan excitation (GP_{exc}^λ) and emission (GP_{em}^λ) generalized polarization, as calculated by Eqs. (1) and (2), respectively, for liposomes of the 1:1 mixture of DMPC and DPPC, at various temperatures. The quasi-linear behavior of spectra is evident. When the slopes of the regression lines are superimposed on the GPS vs. temperature plot obtained by the two-point equations (Eqs. (3) and (4)), the values are fairly coincident as can be observed in panel B, the lower panel of Fig. 2. Only at high temperatures, GP_{exc}^S values calculated by linear regression of GP_{exc}^λ spectra show some deviation from those obtained by the two-point equation. This behavior, which does not affect the general conclusions that can be drawn from the experiment, is attributable to a small departure from linearity of the GP_{exc}^λ spectra at high temperatures and wavelengths longer than 400 nm (curves f–h, Fig. 2A).

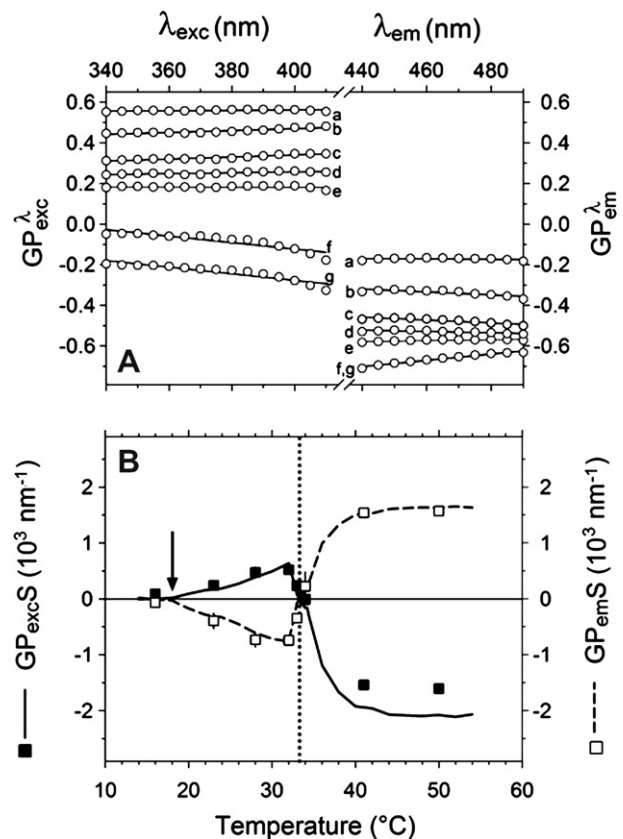


Fig. 2. (A, upper panel) Excitation (GP_{exc}^λ) and emission (GP_{em}^λ) generalized polarization spectra of Laurdan in 1:1 DMPC–DPPC liposomes at different constant temperatures: (a) 16 °C; (b) 28 °C; (c) 32 °C; (d) 33 °C; (e) 34 °C; (f) 41 °C; (g) 50 °C. Data points corresponding to GP spectra at 23 and 33.9 °C were omitted for the sake of clarity. GP_{exc}^λ and GP_{em}^λ values were obtained according to Eqs. (1) and (2), respectively. The lines, which represent the GP spectra, were fitted to data using linear regression analysis. The slopes of the regression lines are represented by the squares in panel B, the lower panel B) Effect of temperature on GP_{exc}^S (—, ■) and GP_{em}^S (---, □) of Laurdan in 1:1 DMPC–DPPC liposomes. GP_{exc}^S and GP_{em}^S are represented by the continuous and dashed lines, respectively, when calculated through Eqs. (3) and (4) or by full or open squares, when obtained from the slopes of the regression lines of the GP data of panel A, the upper panel. The vertical, dotted line corresponds to $T_c = 33.3$ °C. The arrow shows $T_o = 18.1$ °C. Results are the means ($\pm SD$) of three experiments. Standard deviation bars smaller than symbols are not shown.

The thermotropic response of DMPC–DPPC liposomes at various mole fractions of the components was further investigated by means of GP_{exc}^S and GP_{em}^S , as illustrated in Fig. 3. The profiles look similar to those of Figs. 1 and 2B. As already indicated, the vertical dotted lines denote T_c , the temperature marking the apparent limit between phase coexistence and liquid-crystalline state for each phospholipid or phospholipid mixture. The arrows correspond to T_o , the limit between the gel and the coexistence region. Table 1 shows the T_o and T_c values for the different DMPC–DPPC mole fractions employed. It can be observed that as X_{DMPC} decreases, T_o and T_c increase. The values of T_c vary from 24.1 °C for $X_{DMPC} = 1$ to 41.5 °C for $X_{DMPC} = 0$ (i.e., for pure DPPC liposomes).

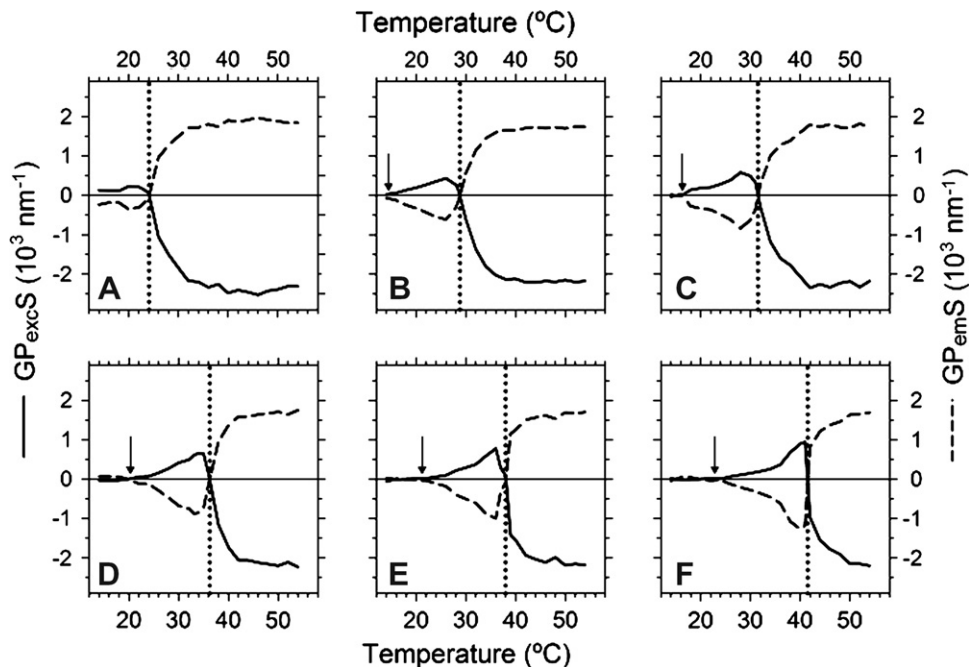


Fig. 3. Effect of temperature on $GP_{exc}S$ (—) and $GP_{em}S$ (---) of Laurdan in DMPC–DPPC liposomes at various constant mole fractions: (A) $X_{DMPC} = 1$; (B) $X_{DMPC} = 0.75$; (C) $X_{DMPC} = 0.625$; (D) $X_{DMPC} = 0.375$; (E) $X_{DMPC} = 0.25$; (F) $X_{DMPC} = 0$ (i.e., $X_{DPPC} = 1$). Calculation of $GP_{exc}S$ and $GP_{em}S$, represented schematically by the continuous and dashed lines, respectively, was done through Eqs. (3) and (4). T_o , the limit between gel and phase coexistence region and T_c , the temperature marking the apparent limit between phase coexistence and liquid-crystalline state, are indicated by the arrows and the vertical dotted lines, respectively, and appear listed in Table 1.

Table 1

T_c and T_o values estimated from Laurdan GPS vs. temperature plots, for DMPC–DPPC mixed liposomes, at various constant phospholipid compositions

X_{DMPC}	T_c (°C)	T_o (°C)
1.000	24.1 ± 0.3	—
0.750	28.8 ± 0.0	14.3 ± 0.4
0.625	31.5 ± 0.3	16.8 ± 0.1
0.500	33.3 ± 0.3	18.1^*
0.375	36.3 ± 0.3	20.2^*
0.250	38.0 ± 0.2	21.3 ± 1.2
0.000	41.5 ± 0.0	23.0 ± 6.1

The table was constructed from plots similar to those shown in Figs. 1, 2B and 3 where the vertical dotted lines and the arrows indicate T_c and T_o , respectively. Results shown are the means ($\pm SD$) of three experiments, except for the values marked with an asterisk (*) which correspond to the average of two experiments.

Likewise, T_o increases from 14.3 to 23 °C in going from $X_{DMPC} = 0.75$ to pure DPPC. This means that the GPS thermotropic profile is displaced along the temperature axis toward higher temperatures, as the proportion of DPPC increases.

Detection of the compositional phase change of DMPC–DPPC mixed liposomes by Laurdan GPS

Another purpose of this study was to determine whether GPS is sensitive to compositional induced phase changes in DMPC–DPPC liposomes. If this were the case, one would

expect GPS vs. composition plots to exhibit, at appropriate temperatures, characteristic points X_o and X_c representing phase boundaries equivalent to T_o and T_c in GPS thermotropic profiles. To explore this possibility, the GPS dependence on the change in composition of DMPC–DPPC vesicles at constant temperature has been studied both, by application of the two-point equations (Eqs. (3) and (4)), and by determination of the GP spectra slopes. Results are presented in Fig. 4 where the upper panel (4A) displays Laurdan excitation (GP_{exc}^λ) and emission (GP_{em}^λ) generalized polarization spectra, as calculated by Eqs. (1) and (2), respectively, for liposomes containing variable proportions of DMPC and DPPC at 34 °C. The GP_{exc}^λ and GP_{em}^λ spectra were subject to linear regression analysis and the slopes of the resulting lines were superimposed on the GPS vs. temperature plot obtained by the two-point equations. Fig. 4B shows that the values obtained by both procedures are nearly coincident except for a few data points at the high DMPC proportions corresponding to the liquid-crystalline state where there is some disagreement. This difference most probably arises from the slight deviation from linearity of the GP_{exc}^λ spectra at high DMPC concentrations and wavelengths longer than 400 nm. However, neither the distinctive features of the GPS profile, nor the general interpretation of the experiment, are affected by this behavior. An important feature of Fig. 4B is the composition point X_c marking the apparent limit between phase coexistence and liquid-crystalline state. Similarly to T_c , this point is very well defined since it corresponds to

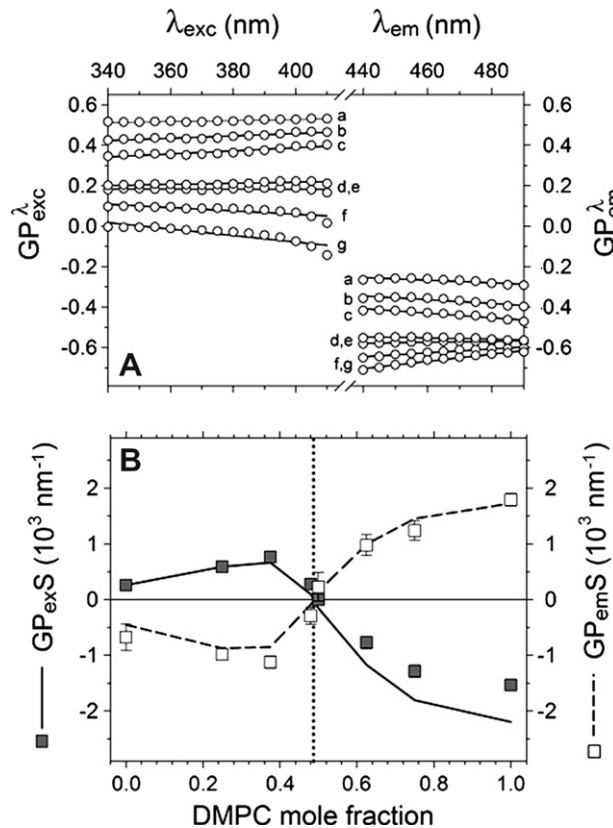


Fig. 4. (A) Excitation (GP_{em}^{λ}) and emission (GP_{em}^{λ}) generalized polarization spectra of Laurdan in DMPC–DPPC liposomes at 34 °C. Liposome composition was as follows: (a) $X_{\text{DMPC}} = 0$; (b) $X_{\text{DMPC}} = 0.25$; (c) $X_{\text{DMPC}} = 0.375$; (d) $X_{\text{DMPC}} = 0.48$; (e) $X_{\text{DMPC}} = 0.50$; (f) $X_{\text{DMPC}} = 0.625$; (g) $X_{\text{DMPC}} = 1$. Data points corresponding to GP spectra at $X_{\text{DMPC}} = 0.75$ were omitted for the sake of clarity. $GP_{\text{exc}}^{\lambda}$ and GP_{em}^{λ} were obtained according to Eqs. (1) and (2), respectively. The lines representing the GP spectra were fitted to data by linear regression analysis. The slopes of the regression lines are represented by the squares in panel B, the lower panel. (B) Laurdan GP_{excS} (—, ■) and GP_{emS} (---, □) as a function of X_{DMPC} (or X_{DPPC}) for DMPC–DPPC liposomes at 34 °C. GP_{excS} and GP_{emS} are represented schematically by the continuous and dashed lines, respectively, when calculated through Eqs. (3) and (4) or by full or open squares, when obtained from the slopes of the GP spectra of panel A, the upper panel. The vertical, dotted line corresponds to $X_{\text{c,DMPC}} = 0.49$ and represents the mole fraction marking the apparent limit between phase coexistence and liquid-crystalline state for the binary mixture at 34 °C. Results are the means ($\pm \text{SD}$) of three experiments. Standard deviation bars smaller than symbols are not shown.

the sharp intersection of GP_{excS} and GP_{emS} with the abscissa. As marked by the vertical, dotted line, $X_{\text{c,DMPC}}$ is equal to 0.49. For $X_{\text{DMPC}} < 0.49$, GP_{excS} is positive and GP_{emS} negative, as expected for coexisting phases. For $X_{\text{DMPC}} > 0.49$, GP_{excS} is negative and GP_{emS} positive, meaning liquid-crystalline state. It is also important to note that at 34 °C, the GPS vs. composition plot does not show the gel region or the point X_o marking the limit between the gel phase and the phase coexistence region. These features only show up at lower experimental temperatures, as described below.

Fig. 5 shows that depending on the temperature employed, different parts of the GPS vs. composition pro-

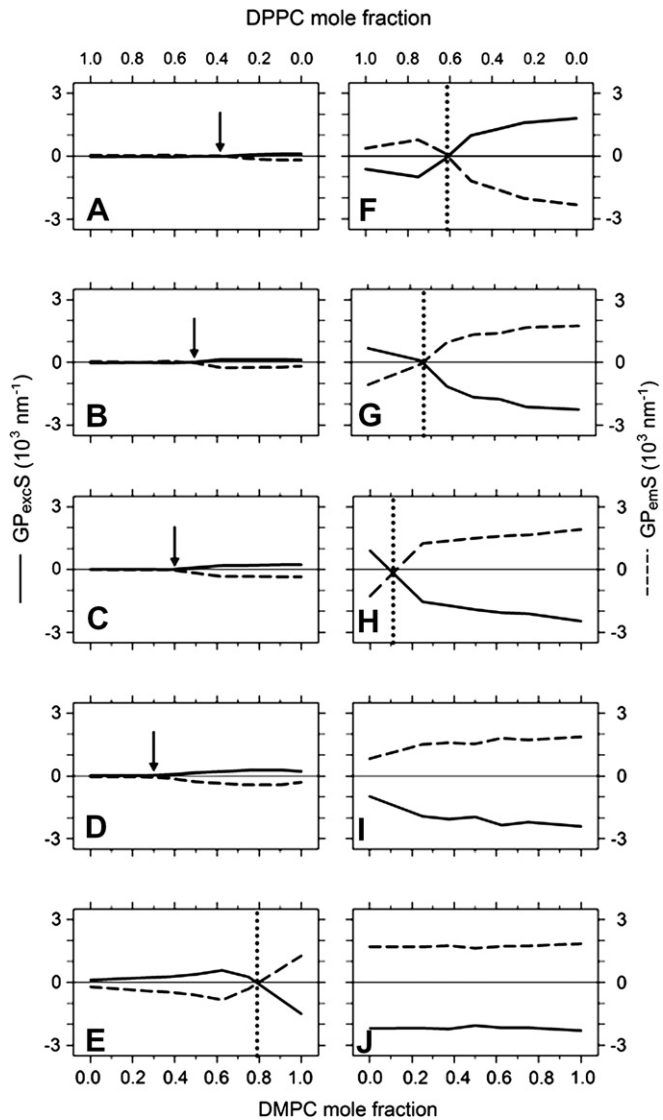


Fig. 5. Laurdan GP_{excS} (—) and GP_{emS} (---) as a function of X_{DMPC} (or X_{DPPC}) for DMPC–DPPC liposomes at different constant temperatures: (A) 16 °C; (B) 18 °C; (C) 20 °C; (D) 22 °C; (E) 28 °C; (F) 36 °C; (G) 38 °C; (H) 40 °C; (I) 42 °C; (J) 54 °C. GP_{excS} and GP_{emS} are represented schematically by the continuous and dashed lines, respectively, and were calculated through Eqs. (3) and (4). Where present, X_o , the phospholipid mole fraction marking the limit between the gel and the phase coexistence regions and X_c , the phospholipid mole fraction corresponding to the limit between phase coexistence and liquid-crystalline state, are indicated by the arrows and the vertical dotted lines, respectively. Their values, expressed in terms of X_{DMPC} , are listed in Table 2.

file are obtained. At low temperature (16 °C, panel A) GP_{excS} and GP_{emS} are equal to zero in most of the composition range, as expected for the gel phase. At high temperature (54 °C, panel J) GP_{excS} is negative and GP_{emS} positive throughout the whole composition range, a behavior corresponding to the liquid-crystalline state. As temperature increases from 16 °C (panel A) to 54 °C (panel J) different, characteristic portions of the profile gradually appear. In this way, from a profile typical of gel phase at low temperature, the system evolves to a profile

characteristic of liquid-crystalline state at high temperature. In the different panels of Fig. 5, the vertical dotted lines and the arrows indicate, where present, the composition points $X_{o,DMPC}$ and $X_{c,DMPC}$, respectively. Their values are listed in Table 2 which shows that as temperature increases, $X_{o,DMPC}$ and $X_{c,DMPC}$ decrease. That is, the higher the temperature, the larger the mole fraction of

Table 2
 $X_{c,DMPC}$ and $X_{o,DMPC}$ values estimated from Laurdan GPS vs. composition plots for DMPC-DPPC mixed liposomes, at various constant temperatures

T (°C)	X_c , DMPC	X_o , DMPC
14.0	—	0.763 ± 0.075
16.0	—	0.617 ± 0.141
18.0	—	0.493 ± 0.039
20.0	—	0.400 ± 0.000
22.0	—	0.300 ± 0.010
24.0	—	0.127 ± 0.115
26.0	0.837 ± 0.010	—
28.0	0.793 ± 0.011	—
30.0	0.688 ± 0.009	—
32.0	0.591 ± 0.016	—
34.0	0.490 ± 0.020	—
36.0	0.387 ± 0.013	—
38.0	0.255 ± 0.029	—
40.0	0.109 ± 0.010	—

The table was constructed from plots similar to those shown in Figs. 4B and 5, where the vertical dotted lines and the arrows indicate X_c and X_o , respectively. Results shown are the means (\pm SD) of three experiments.

DPPC (which is the longer-chained phosphatidylcholine in the binary mixture) at the composition points X_o and X_c . It should be mentioned that the point X_o , at the edge of the gel phase, cannot be identified as clearly as X_c because the change from the gel phase to the coexistence region occurs smoothly. This is the cause of the much larger standard deviations shown by X_o values as compared to X_c values.

An important, general conclusion from this part of the results is that under constant temperature conditions, GPS is clearly sensitive to the phase transition induced by changes in the proportion of DMPC and DPPC in the two-component liposomes.

Discussion

We have found that Laurdan GPS is sensitive to the thermotropic and compositional phase changes of DMPC-DPPC liposomes. On one hand, the thermotropic GPS profiles yield characteristic transition temperatures T_o and T_c . On the other, GPS detects composition-induced phase changes at specific mole fractions X_o and X_c . The representation and analysis of our results in terms of a temperature-composition phase diagram can furnish further information on the physical meaning of T_o , T_c , X_o and X_c by comparison with diagrams constructed from other methodological approaches [4,20].

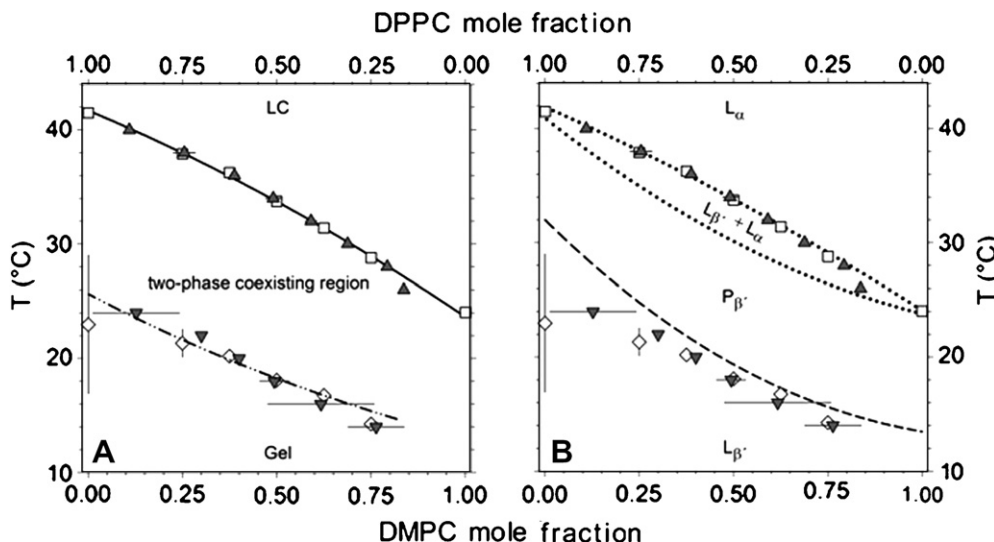


Fig. 6. Temperature-composition diagrams for DMPC-DPPC liposomes. (A, left panel) GPS-derived diagram showing the boundaries of the two-phase coexisting region with the liquid-crystalline state (—) and the gel phase (—·—·—). The diagram was generated from Laurdan GPS-derived parameters, as listed in Tables 1 and 2. The open squares (\square) correspond to T_c (data from Table 1) and the full triangles (\blacktriangle) to X_c (data from Table 2). The solid line drawn through these points shows the boundary between the two-phase coexisting region and the liquid-crystalline phase. The dash-dot-dotted line has been traced through the points corresponding to T_o (\diamond) (mean values and SD's from Table 1) and X_o (\blacktriangledown) (mean values and SD's from Table 2) and shows the limit between the gel phase and the coexistence region. Both the solid and dash-dot-dotted lines were fitted to data by second order polynomial regression. (B, right panel) X_c , T_c , X_o and T_o , the GPS-based data points of the left panel, displayed superimposed over a DMPC-DPPC schematic phase diagram showing L_α , P_β^+ and L_β^+ phase equilibria, as adapted from Mabrey and Sturtevant [4] and Matubayasi et al. [20]. The dotted curves (···), drawn through data points taken from Mabrey and Sturtevant [4], stand for the solidus and fluidus lines (lower and upper curve, respectively), representing the temperatures of onset and completion of the main phase change, in the order mentioned. The dashed line (---) has been drawn through data points of Matubayasi et al. [20] and marks the boundary between the L_β^+ phase and P_β^+ , the ripple phase. Both, the dotted and dashed lines were fitted to data by second order polynomial regression.

Fig. 6A shows the partial temperature–composition phase diagram for the DMPC–DPPC mixtures, generated from the T_c and T_o values listed in **Table 1** as well as the X_c and X_o data listed in **Table 2**. The diagram reflects the agreement between results obtained from GPS vs. temperature and GPS vs. composition plots. It can be observed that the T_c and X_c values lie along a single line marking the apparent limit between the liquid-crystalline and the phase coexistence regions. Likewise, the T_o and the X_o values lie along another single line defining the apparent boundary between the phase coexistence region and the gel phase.

The phase behavior of DMPC–DPPC lamellar systems has been investigated previously by different methodologies including electron spin resonance [5], differential scanning calorimetry [4,20,40], nuclear magnetic resonance [38], vesicle permeability [39] and theoretical modeling [21,37,41], among others. Particularly worth of mention is the calorimetric study of Mabrey and Sturtevant [4] which has repeatedly been taken as a reference for the assessment of main phase transition results [20,21,37–41]. We have also selected the DMPC–DPPC phase diagram from the same work as a term of comparison for our main phase transition data. Such diagram, however, does not include the pretransition, i.e., the change from the gel to ripple phase. For this, we turned to the pretransition data of Matubayasi et al. [20]. These authors used calorimetric and optical absorbance methods to perform a thermotropic study of the pretransition and the main phase transition of liposomes composed of a range of DMPC–DPPC mixtures. In **Fig. 6B**, and for comparison, the GPS-based data points of **Fig. 6A** are displayed superimposed on a DMPC–DPPC phase diagram adapted from the above-mentioned publications [4,20] and showing the L_α (liquid crystalline), P_β' (ripple) and L_β' (gel) phase equilibria. In the diagram, the dotted curves have been drawn through data points taken from Mabrey and Sturtevant [4] and stand for the *solidus* and *fluidus* lines (lower and upper curve, respectively), representing the temperatures of onset and completion of the main phase change, respectively [4,22]. In addition, a dashed line drawn through data points from Matubayasi et al. [20] marks the limit between the L_β' and P_β' phases. It can be observed that the T_c and X_c points obtained from the GPS vs. temperature and GPS vs. composition plots, respectively, fall almost exactly over the *fluidus* line indicating that they define the completion of the gel to liquid-crystalline main phase transition process. In contrast, and according to our results, Laurdan does not report the onset of the gel–liquid-crystalline main phase transition, that is, it cannot be employed to draw the *solidus* line in a temperature–composition phase diagram (**Figs. 6A** and **B**). In fact, the T_o and X_o points, which define the onset of the transition process in a GPS heating scan, fall very far below the *solidus* line and even below but near the limit between the L_β' and the P_β' (ripple) phases [20]. The region within the T_o/X_o and T_c/X_c boundaries corresponds to positive $GP_{exc}S$ and negative $GP_{em}S$ values which are characteristic

of the coexistence of gel and liquid-crystalline domains. Interestingly, such region includes the rippled phase reported in the literature [20]. This phase seems to be favored by the presence of Tris buffer at concentrations of 20–50 mM, as shown by atomic force microscopy images of mica-supported bilayers [42]. In the case of the present study, experiments were carried out at 10 mM Tris, a concentration too small to be the cause of the observed ripple phase [43].

Our GPS results on the rippled state are in agreement with the suggestion that in such a phase, gel phospholipids coexist with a fraction of L_α phospholipids. According to an electron spin resonance (ESR) investigation of DPPC liposomes performed several years ago by Tsuchida and Hatta [44], the molecular organization of the ripple phase could be explained by the coexistence of the ordered lipids of the L_β' phase and the disordered lipids of the L_α phase. More recently, Rappolt et al. [45] reported that time-resolved X-ray diffraction data also supported the proposal that gel and liquid-crystalline phases coexisted in the ripple state of phosphatidylcholine membranes. Likewise, based on Monte Carlo simulations, Heimburg has hypothesized that the ripple phase is composed of periodic arrangements of fluid line defects in a gel lipid matrix [9]. Many other studies point to the non-homogeneous structure of the P_β' phase. For instance, X-ray scattering and electron density maps from Sun et al. seem to indicate that the major side of DMPC ripples corresponds to a gel phase lipid bilayer while the minor side is thinner and more consistent with a fluid L_α bilayer [8]. Another model derived from molecular dynamics simulations of DPPC bilayers proposes that the ripple phase consists of gel-like and splayed gel domains, separated by disordered lipids [46].

It has been mentioned above that most of our X_o and T_o data points are near, but below, the gel–ripple line reported by Matubayasi et al. [20] with the larger differences corresponding to liposomes containing the higher proportions of DPPC (**Fig. 6B**). This discrepancy can be accounted for by the relatively large standard deviations of the T_o and X_o data. As previously indicated, these parameters cannot be determined as precisely as T_c and X_c . Nevertheless, the deviation found between the T_o/X_o boundary and the gel–ripple line hardly affects the two main conclusions drawn from the phase diagrams in **Fig. 6**, which can be summarized as follows. First, while the T_c/X_c boundary is coincident with the *fluidus* line [4,22], the T_o/X_o boundary does not correspond to the *solidus* line defining the onset of the main phase transition [4,22]. Second, the ripple-phase zone is part of an area corresponding to the coexistence of gel and liquid-crystalline phases, as identified by Laurdan GPS. In this way, GPS results support the view of a heterogeneous structure for the ripple state [8–10,44–46].

The ability of Laurdan GPS to monitor the phase state of phospholipid membranes [11] has been confirmed, in the present work, by the successful use of GPS-derived parameters to depict a partial phase diagram for mixtures of DMPC and DPPC. A similar approach could be applied

to the analysis of other phospholipid mixtures as well as to the investigation of the effect of cholesterol on the physical properties of phospholipid bilayers. Remarkably, Laurdan GPS allows the identification of the phase coexistence region and the definition of its temperature and composition boundaries. This can potentially be useful in investigations of one of the most interesting aspects of lipid phase behavior, namely, the domain formation in biomembranes [19,47,48].

There are other possible biological applications of this investigation that can be analyzed in the context of previous work of our laboratory [11,49,50]. In an introductory study of the GPS function, we employed liposomes from *E. coli* lipid extracts consisting of a mixture of three main components: phosphatidylethanolamine, phosphatidylglycerol and cardiolipin [11,51]. For Laurdan incorporated in vesicles of this phospholipid mixture, the GPS thermotropic profile showed marked shifts along the temperature axis, depending on the growth temperature of the bacteria from which the extracts were obtained. The shifts can be related to the increase in the ratio of saturated to unsaturated fatty acyl chains that takes place in membrane phospholipids, as growth temperature is raised [11,49–51]. Remodeling of phospholipid acyl chains has a profound effect on microfluidity and is the origin of membrane homeoviscous regulation [49,50]. A study of the effect of these phenomena on the phase behavior of *E. coli* membranes may be implemented based on the detailed characterization of the GPS capacity to detect phase transitions, described here. It would be interesting to compare results from bacteria grown in steady-state at different temperatures with those exposed to sudden thermal stress [49,50]. The investigations could be performed not only on isolated membranes but also on membranes of *E. coli* whole cells into which Laurdan can be incorporated [47]. Besides, it is reasonable to expect that the characteristic features of the GPS function discussed in the present work, will provide more information than the generalized polarization [47], about the presence of membrane heterogeneities in bacteria.

Overall, our results suggest that the GPS function can be used as a reliable, quantitative tool to investigate the lateral organization of single phospholipids and phospholipid mixtures in bilayers. This novel approach might open up new perspectives for model system and natural membrane studies, based on Laurdan fluorescence spectroscopy.

Acknowledgment

This work will be part of the Doctor of Science Thesis of A.A. Vallejo, who is the recipient of a fellowship from CONACyT (México).

References

- [1] G. Vereb, J. Szöllősi, J. Matkó, P. Nagy, T. Farkas, L. Vígh, L. Mátyus, T.A. Waldmann, S. Damjanovich, Proc. Natl. Acad. Sci. USA 100 (2003) 8053–8058.
- [2] B. Brugger, B. Glass, P. Haberkant, I. Leibrecht, F.T. Wieland, H.G. Krausslich, Proc. Natl. Acad. Sci. USA 103 (2006) 2641–2646.
- [3] J. Korlach, P. Schwille, W.W. Webb, G.W. Feigenson, Proc. Natl. Acad. Sci. USA 96 (1999) 8461–8466.
- [4] S. Mabrey, J.M. Sturtevant, Proc. Natl. Acad. Sci. USA 73 (1976) 3862–3866.
- [5] E.J. Shimshick, H.M. McConnell, Biochemistry 12 (1973) 2351–2360.
- [6] J.H. Ipsen, K. Jørgensen, O.G. Mouritsen, Biophys. J. 58 (1990) 1099–1107.
- [7] O.G. Mouritsen, K. Jørgensen, Chem. Phys. Lipids 73 (1994) 3–25.
- [8] W.J. Sun, S. Tristram-Nagle, R.M. Suter, J.F. Nagle, Proc. Natl. Acad. Sci. USA 93 (1996) 7008–7012.
- [9] T. Heimburg, Biophys. J. 78 (2000) 1154–1165.
- [10] M. Kranenburg, B. Smit, J. Phys. Chem. B 109 (2005) 6553–6563.
- [11] J.B. Velázquez, M.S. Fernández, Arch. Biochem. Biophys. 455 (2006) 163–174.
- [12] M.S. Fernández, M.T. González-Martínez, E. Calderón, Biochim. Biophys. Acta 863 (1986) 156–164.
- [13] M.S. Fernández, Biochim. Biophys. Acta 646 (1981) 23–26.
- [14] M.S. Fernández, E. Calderón, Ber. Bunsenges. Phys. Chem. 95 (1991) 1669–1674.
- [15] M.T. González-Martínez, M.S. Fernández, Biochem. Biophys. Res. Commun. 151 (1988) 851–858.
- [16] M.S. Fernández, R. Mejía, E. Zavala, Biochem. Cell Biol. 69 (1991) 722–727.
- [17] M.S. Fernández, J.A. Juárez, Biochim. Biophys. Acta 1192 (1994) 132–142.
- [18] R. Morales, M.S. Fernández, Arch. Biochem. Biophys. 398 (2002) 221–228.
- [19] C. Leidy, O.G. Mouritsen, K. Jørgensen, G.H. Peters, Biophys. J. 87 (2004) 408–418.
- [20] N. Matubayasi, T. Shigematsu, T. Ihara, H. Kamaya, I. Ueda, J. Membr. Biol. 90 (1986) 37–42.
- [21] J.H. Ipsen, O.G. Mouritsen, Biochim. Biophys. Acta 944 (1988) 121–134.
- [22] C. Johann, P. Garidel, L. Mennicke, A. Blume, Biophys. J. 71 (1996) 3215–3228.
- [23] T. Parasassi, M. Loiero, M. Raimondi, G. Ravagnan, E. Gratton, Biochim. Biophys. Acta 1153 (1993) 143–154.
- [24] T. Parasassi, E.K. Krasnowska, L. Bagatolli, E. Gratton, J. Fluoresc. 8 (1998) 365–373.
- [25] T. Parasassi, E. Gratton, J. Fluoresc. 5 (1995) 59–69.
- [26] T. Parasassi, G. De Stasio, A. d'Ubaldo, E. Gratton, Biophys. J. 57 (1990) 1179–1186.
- [27] T. Parasassi, M. Di Stefano, G. Ravagnan, O. Sapora, E. Gratton, Exp. Cell Res. 202 (1992) 432–439.
- [28] T. Parasassi, G. Ravagnan, R.M. Rusch, E. Gratton, Photochem. Photobiol. 57 (1993) 403–410.
- [29] T. Parasassi, A.M. Giusti, M. Raimondi, E. Gratton, Biophys. J. 68 (1995) 1895–1902.
- [30] T. Parasassi, G. De Stasio, G. Ravagnan, R.M. Rusch, E. Gratton, Biophys. J. 60 (1991) 179–189.
- [31] G. Weber, F.J. Farris, Biochemistry 18 (1979) 3075–3078.
- [32] A.B. Hendrich, O. Wesolowska, K. Michalak, Biochim. Biophys. Acta 1510 (2001) 414–425.
- [33] L.A. Bagatolli, T. Parasassi, G.D. Fidelio, E. Gratton, Photochem. Photobiol. 70 (1999) 557–564.
- [34] S. Mukherjee, A. Chattopadhyay, Biochim. Biophys. Acta 1714 (2005) 43–55.
- [35] F.M. Harris, K.B. Best, J.D. Bell, Biochim. Biophys. Acta 1565 (2002) 123–128.
- [36] M.S. Fernández, Biochim. Biophys. Acta 646 (1981) 27–30.
- [37] K. Jørgensen, M.M. Sperotto, O.G. Mouritsen, J.H. Ipsen, M.J. Zuckermann, Biochim. Biophys. Acta 1152 (1993) 135–145.
- [38] R. Jacobs, E. Oldfield, Biochemistry 18 (1979) 3280–3285.
- [39] T.X. Xiang, B.D. Anderson, Biochim. Biophys. Acta 1370 (1998) 64–76.
- [40] P. Garidel, A. Blume, Biochim. Biophys. Acta 1371 (1998) 83–95.

- [41] R.E. Jacobs, B.S. Hudson, H.C. Andersen, *Biochemistry* 16 (1977) 4349–4359.
- [42] J. Mou, J. Yang, Z. Shao, *Biochemistry* 33 (1994) 4439–4443.
- [43] H.A. Rinia, R.A. Demel, J.P.J.M. van der Eerden, B. de Kruijff, *Biophys. J.* 77 (1999) 1683–1693.
- [44] K. Tsuchida, I. Hatta, *Biochim. Biophys. Acta* 945 (1988) 73–80.
- [45] M. Rappolt, G. Pabst, G. Rapp, M. Kriechbaum, H. Amenitsch, C. Krenn, S. Bernstorff, P. Laggner, *Eur. Biophys. J.* 29 (2000) 125–133.
- [46] A.H. de Vries, S. Yefimov, A.E. Mark, S.J. Marrink, *Proc. Natl. Acad. Sci. USA* 102 (2005) 5392–5396.
- [47] S. Vanounou, D. Pines, E. Pines, A.H. Parola, I. Fishov, *Photochem. Photobiol.* 76 (2002) 1–11.
- [48] S.R. Shaikh, M.A. Edidin, *Chem. Phys. Lipids* 144 (2006) 1–3.
- [49] R. Mejía, M.C. Gómez-Eichelmann, M.S. Fernández, *Arch. Biochem. Biophys.* 368 (1999) 156–160.
- [50] R. Mejía, M.C. Gómez-Eichelmann, M.S. Fernández, *Biochim. Biophys. Acta* 1239 (1995) 195–200.
- [51] J.E. Cronan, C.O. Rock, in: F.C. Neidhart (Ed.), *Escherichia coli and Salmonella: Cellular and Molecular Biology*, ASM Press, USA, 1996, pp. 612–636.